Elastic, anelastic, and piezoelectric coefficients of GaN

Cite as: J. Appl. Phys. **111**, 013509 (2012); https://doi.org/10.1063/1.3674271
Submitted: 27 July 2011 . Accepted: 07 December 2011 . Published Online: 06 January 2012

N. Nakamura, H. Ogi, and M. Hirao

Elastic, anelastic, and piezoelectric coefficients of GaN

N. Nakamura,[a] H. Ogi, and M. Hirao
Graduate School of Engineering Science, Osaka University, Toyonaka, Osaka 560-8531, Japan

(Received 27 July 2011; accepted 7 December 2011; published online 6 January 2012)

We report elastic, anelastic, and piezoelectric coefficients of wurtzite GaN measured by resonant-ultrasound spectroscopy coupled with laser-Doppler interferometry. Five rectangular parallelepiped specimens, measuring $6.5 \times 2.0 \times 4.0$ mm^3, cut from two single crystals were used. Our values of elastic and piezoelectric coefficients were $C_{11} = 359.4$ GPa, $C_{12} = 129.2$ GPa, $C_{13} = 92.0$ GPa, $C_{33} = 389.9$ GPa, $C_{44} = 98.0$ GPa, $e_{15} = 0.10$ C/m^2, $e_{31} = 0.17$ C/m^2, and $e_{33} = 0.29$ C/m^2. In anelastic coefficients, anisotropy was observed between ${Q_{11}}^{-1}$ and ${Q_{33}}^{-1}$.
 [doi:10.1063/1.3674271]

I. INTRODUCTION

Wurtzite gallium nitride (GaN) shows the energy gap of 3.432-3.452 eV at room temperature.[1] This makes this material attractive for optoelectronic applications, such as light emitting diodes and laser diodes. Considering the piezoelectricity, GaN could be applicable for acoustic resonators.[2,3] Single crystal GaN is also used as a substrate, on which nitride materials grow epitaxially.[4] Elastic coefficients C_{ij}, piezoelectric coefficients e_{ij}, and anelastic coefficients Q_{ij}^{-1} are essential for these applications.

C_{ij} and e_{ij} of wurtzite GaN have been measured by several techniques, as described later, but reliable values have not been obtained. The reason is that the piezoelectric stiffening was not taken account in the previous studies. In piezoelectric materials, acoustic waves behave as if the material is stiffened, because of generation of an electric field from the vibrational strain and subsequent generation of a piezoelectric strain.[5] This is called piezoelectric stiffening. Therefore, by measuring acoustic velocities or phonon frequencies, C_{ij} and e_{ij} are, in principle, simultaneously determined. For example, a velocity of a longitudinal acoustic wave propagating in the x_3 direction of GaN, corresponding to the c axis of a point group 6*mm* crystal, is expressed as $v = \sqrt{(C_{33} + e_{33}^2/\epsilon_{33})/\rho}$. In this case, the apparent stiffness is larger than C_{33} by e_{33}^2/ϵ_{33}, where ϵ_{33} is the dielectric coefficient in the x_3 direction and ρ the mass density. The piezoelectric stiffening term is usually smaller than the elastic stiffness, and the contribution to v is 0.2% in GaN. Therefore, to determine the e_{ij}, velocities (or frequencies) have to be measured with high accuracy. However, in the previous studies, this was not achieved, because of the limited sample size. Hence, the piezoelectric stiffening has not been included.

In the past, Savastenko and Sheleg determined C_{ij} using the mean square displacement of GaN atoms measured by the x-ray method.[6] This is the first study that measured C_{ij}. However, their C_{ij} were significantly smaller than those reported in the following studies, and they are questionable. There are several studies that used Brillouin scattering, and a needle-like single crystal of roughly 500 μm along the c axis and 200 μm in diameter,[7] a film with a thickness of 2 μm grown on a sapphire substrate,[8] a film with a thickness of 4 μm grown on a sapphire substrate,[9] and a GaN substrate with a thickness of approximately 70 μm (Ref. 10) were examined. In the Brillouin scattering, the coefficients are determined from the frequency shifts in the scattered light, and the frequency shifts are determined from peak positions in the Brillouin spectra. When small samples are examined, peak heights tend to be lowered, because the incident laser is not scattered sufficiently by the acoustic phonons and it lowers the wavevector selectivity in the Bragg scattering. This results in the lowered measurement accuracy of peak positions. Referring to the Brillouin spectrum measured by Yamaguchi *et al.*,[9] the Q value of a peak was about 20. This is not a sufficiently large value to determine e_{ij}. Schwarz *et al.* measured C_{ij} of a rectangular parallelepiped GaN, measuring $2.010 \times 2.309 \times 0.285$ mm^3, by resonant ultrasound spectroscopy (RUS),[11] which is the same approach as in this study. RUS determines the C_{ij} and e_{ij} from free-vibration resonance frequencies, and accurate measurement of the frequencies is the key point. In the literature, resonance frequencies were measured by holding the sample at two opposite corners by slightly clamping it between two piezoelectric transducers. In this setup, the contacting force at the corners changes the resonance frequencies to some extent, especially for a small specimen, such as the one used by them, and improvement of the setup is indispensable to determine C_{ij} and e_{ij} simultaneously. Deger *et al.* measured C_{ij} of GaN film of 800-1300 nm thick deposited on sapphire substrates from the velocity dispersion of the surface acoustic wave (SAW).[12] SAW was generated and detected using aluminum integrated transducers (IDT). In this case, ambiguity of the boundary condition at the surface is caused by the fabrication of the IDT, and the strong effect of the substrate's C_{ij} and e_{ij} prevents one from deducing the e_{ij} of the GaN film. Thus, the piezoelectric stiffening has been omitted in the determination of C_{ij}. Regarding e_{ij}, the value was estimated by Bykhovski[13] from the data on electromechanical coupling coefficients that was measured using the SAW by O'Clock and Duffy.[14] Guy *et al.*[15] and Lueng *et al.*[16] measured e_{ij} of the GaN film on several substrates by the interferometric technique. However, the determination of e_{ij} is generally more difficult than C_{ij}, and the values are still ambiguous. Regarding Q_{ij}^{-1}, there are no reports.

[a]Electronic mail: nobutomo@me.es.osaka-u.ac.jp.

Thus, the complete set of C_{ij} and e_{ij} of GaN has not been determined simultaneously. In this study, we achieve this and report the complete set of C_{ij}, e_{ij}, and Q_{ij}^{-1} of wurtzite GaN. This was made possible by resonant-ultrasound spectroscopy coupled with laser-Doppler interferometry (RUS/LDI).[17] In piezoelectric materials, free-vibration resonance frequencies are affected by dimensions, mass density, C_{ij}, e_{ij}, and ϵ_{ij}. Therefore, measurement of resonance frequencies of a specimen, whose dimensions, mass density, and ϵ_{ij} are known, can deduce a complete set of C_{ij} and e_{ij} using the Ritz method. This approach was suggested by Ohno[18] and Dunn *et al.*,[19] but was not actualized because of the small contributions of e_{ij} and difficulties in mode identification. We developed the needle-transducer tripod to measure the resonance frequencies of small specimens with sufficiently high accuracy to determine C_{ij} as well as e_{ij}. Furthermore, we used laser-Doppler interferometry (LDI) to identify the vibrational modes unambiguously. We call this method the RUS/LDI method and have applied it to quartz,[20] langasite,[21] lithium niobate,[22] and TeO_2.[23] The reliability of the RUS/LDI has been verified by comparing it to other methods. Once C_{ij} is determined, Q_{ij}^{-1} is determined from the contribution of C_{ij} on resonance frequency, $\partial f/\partial C_{ij}$, and internal friction, Q^{-1}, of each resonance frequency measured from the half width of the resonance peak.[21]

One of the advantages of the RUS/LDI method over other acoustic methods is that the complete set of coefficients is determined simultaneously from a single specimen. In a typical acoustic method, several specimens, which are cut in different crystallographic orientations, were required to determine all the independent coefficients.[24,25] Then, orientation error and dimension error are accumulated in the resultant coefficients. Another advantage is that C_{ij} and e_{ij} are determined from a large number of the resonance frequencies, that is, redundancy. In typical acoustic methods, to determine several independent coefficients, the same number of frequencies (or velocities) are measured. However, in the RUS/LDI, the number of the measured frequency is much larger than the unknown coefficients; we measure more than sixty resonance frequencies for eight coefficients in GaN and determine the coefficients using the least square fitting, thus increasing the accuracy. For these reasons, we consider that the RUS/LDI deduces the reliable coefficients compared to other methods.

In this study, we use five specimens, and five independent sets of the C_{ij} and e_{ij} are determined. Then, the measurement accuracy is thoroughly evaluated. Furthermore, the specimens are significantly larger than those used in the previous studies. Considering that a single set of the coefficients has been determined from small specimens so far, the present study should give more reliable coefficients than previous studies.

II. EXPERIMENTAL DETAILS

Two GaN crystals were provided by Mitsubishi Chemical Corporation. Carrier density measured by van der Pauw method was 2.2×10^{17} and $9.3 \times 10^{17}\,\mathrm{cm}^{-3}$. Four rectangular parallelepiped specimens were cut out from the former crystal and one from the latter. Typical edge lengths were 4.0 mm in the c axis and 6.5 and 2.0 mm in perpendicular directions. Specimen dimensions were measured using a micrometer. Using Archimedes' method and distilled water as a standard, we found a mass density $\rho = 6.070\,\mathrm{g/cm}^3$.

Hexagonal GaN belonging to the point group $6mm$ shows five independent elastic-stiffness coefficients (C_{11}, C_{12}, C_{13}, C_{33}, C_{44}),

$$[C_{ij}] = \begin{bmatrix} C_{11} & C_{12} & C_{13} & 0 & 0 & 0 \\ C_{12} & C_{11} & C_{13} & 0 & 0 & 0 \\ C_{13} & C_{13} & C_{33} & 0 & 0 & 0 \\ 0 & 0 & 0 & C_{44} & 0 & 0 \\ 0 & 0 & 0 & 0 & C_{44} & 0 \\ 0 & 0 & 0 & 0 & 0 & \dfrac{C_{11}-C_{12}}{2} \end{bmatrix}. \quad (1)$$

It shows three independent piezoelectric coefficients (e_{15}, e_{31}, e_{33}),

$$[e_{ij}] = \begin{bmatrix} 0 & 0 & 0 & 0 & e_{15} & 0 \\ 0 & 0 & 0 & e_{15} & 0 & 0 \\ e_{31} & e_{31} & e_{33} & 0 & 0 & 0 \end{bmatrix} \quad (2)$$

and two independent dielectric coefficients (ϵ_{11}, ϵ_{33}),

$$[\epsilon_{ij}] = \begin{bmatrix} \epsilon_{11} & 0 & 0 \\ 0 & \epsilon_{11} & 0 \\ 0 & 0 & \epsilon_{33} \end{bmatrix}. \quad (3)$$

In the RUS/LDI, elastic stiffness coefficients at constant electric field C_{ij}^E and dielectric coefficients at constant strain ϵ_{ij}^S are considered. In this paper, we use the simplified notation as C_{ij} and ϵ_{ij}, respectively. All the coefficients contribute to free-vibration resonance frequencies, but e_{ij} and ϵ_{ij} cannot be separated, because only their combinations affect the resonance frequencies. We then used the reported values[26,27] $\epsilon_{11}/\epsilon_0 = 5.35$ and $\epsilon_{33}/\epsilon_0 = 5.8$, where ϵ_0 denotes the vacuum permittivity.

In the following, we discuss measurement accuracy of the resultant coefficients. Possible error sources are measurement errors in the resonance frequencies, dimensions, and mass density and also calculation error with the Ritz method. First, we consider the calculation error. In the RUS/LDI, free vibration of a rectangular parallelepiped is analyzed by the Lagrangian minimization. By combining with the least-squares fitting procedure, a set of the coefficients are determined from the resonance frequencies. Because no analytical solution exists for the displacements and electric potential in a piezoelectric rectangular-parallelepiped specimen subjected to a free vibration, they are approximated by linear combinations of basis functions. In this study, Legendre functions[28] are used. Use of higher-order basis functions leads to increase the accuracy of resonance frequencies, but it takes a longer calculation time. After calculating resonance frequencies with various maximum order of the basis function, N, up to 26, we decided to use $N = 18$. The calculation errors in the frequencies were then less than 0.0045%, being significantly smaller than the measurement errors. Therefore, the calculation error is negligible. Details of the evaluation procedure are described elsewhere.[20]

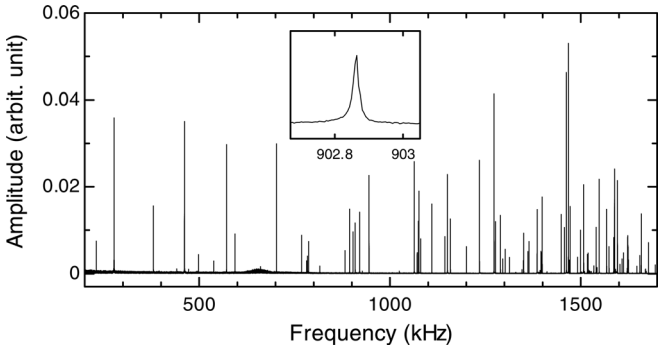

FIG. 1. Resonance spectrum of a specimen measured in a vacuum. Inset shows an enlarged resonance peak.

Resonance frequencies are measured by the tripod transducer set in a vacuum chamber. The tripod transducer is composed of two piezoelectric pinducers and a thermocouple. A specimen is placed on the tripod. Then, no external force was applied to the specimen except for gravity. The resonance frequencies were measured at $30 \pm 0.5\,^{\circ}\mathrm{C}$ three times for each specimen to see the reproducibility; after measuring the resonance frequencies, we took the specimen out of the vacuum chamber, replaced it on the tripod, and again measured the frequencies in vacuum. Standard deviations of the resonance frequencies among the completely independent three measurements were smaller than 0.06%, regardless of the different contact points between the specimen and the needles. Figure 1 shows an example of the measured resonance spectrum.

We usually deduce C_{ij} and e_{ij} of each specimen using the average values of the resonance frequencies from a number of measurements. However, we here deduced three sets of C_{ij} and e_{ij} of a specimen using each set of the resonance frequencies to evaluate the errors in the resultant coefficients caused by the fluctuation of the resonance frequencies. Table I shows the standard deviation of the coefficients. The deviations were different for each coefficient, and e_{ij}, especially e_{31}, showed a large error. Considering the contribution to the resonance frequencies, this can be consistently interpreted. The contribution is defined as $|p/f(\partial f/\partial p)|$, where p is one of C_{ij} and e_{ij} and it is calculated by the Ritz method, as shown in Fig. 2. In the figure, the contribution of e_{ij} was significantly smaller than those of C_{ij}, and e_{31} showed the smallest contributions. Measurement error in C_{ij} and e_{ij} caused by the measurement error in the resonance frequency was nearly proportional to the inverse of the contribution values, and this result indicates that the resultant error by the resonance frequency depends on the contributions.

Measurement error in the dimension with a micrometer was $\pm 1\mu$m. To evaluate the influence, we deduced C_{ij} and

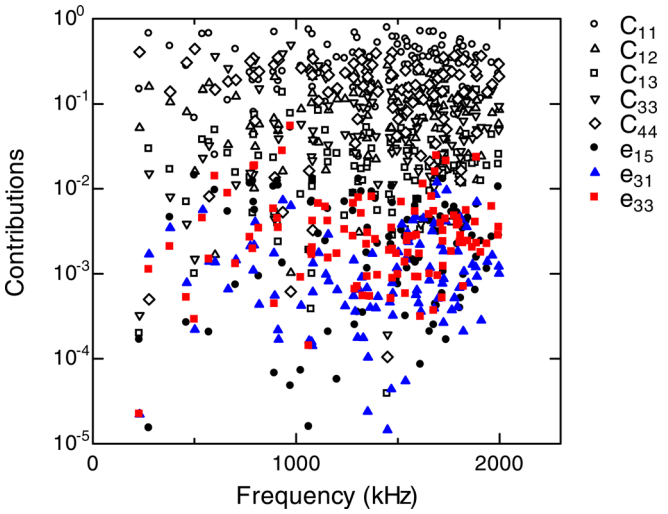

FIG. 2. (Color online) Normalized contributions of C_{ij} and e_{ij} to resonance frequencies.

e_{ij} by adding $1\,\mu$m to every edge lengths, corresponding to 0.09% change in volume. The calculation result is shown in Table I. The errors in C_{ij} and e_{ij} showed the same behavior as those by the frequency fluctuation; the errors in e_{ij} were larger than those in C_{ij}. Considering that resonance frequencies possess different sensitivity to dimensions, it is obvious that C_{ij} and e_{ij} determined from the resonance frequencies show different sensitivity to the dimension errors. Usage of specimens having different dimensions from present specimens may modify the sensitivities, and errors in the resultant e_{ij} caused by dimension errors could be improved.

In Archimedes' method, measurement accuracy of a microbalance affects the measurement error of the mass density, and it was 0.09%. Similarly to the analysis done for the dimension error, C_{ij} and e_{ij} were deduced assuming that the mass density was increased by 0.09%. In this case, the errors in C_{ij} were comparable to the density error as seen in Table I. Considering that contribution of mass density ρ to resonance frequencies is independent of the vibrational mode and the frequencies are generally proportional to $\sqrt{C_{ij}/\rho}$, resultant C_{ij} should be proportional to ρ. Regarding e_{ij}, the error differs for each e_{ij}, because the piezoelectric stiffening term e^2/ϵ is affected by ρ, and the contribution of ρ to the resultant e_{ij} cannot be described as simply as for C_{ij}. Thus, we confirmed that the measurement error in C_{ij} was up to 0.30% and that in e_{ij} ranged from 5.5 to 117%, which was deduced from the sum of the errors of coefficients shown in Table I.

In the inverse calculation, we must make the one-to-one correspondence between measured and calculated resonance frequencies. The vibrational modes of calculated resonance frequencies are known, but those of observed resonance peaks

TABLE I. Errors (%) in C_{ij} and e_{ij} caused by the fluctuation of resonance frequency among three independent measurements Δf (0.06%) and measurement errors in mass density $\Delta\rho$ (0.09%) and dimension Δd (adding 1 μm in edge lengths, corresponding to volume change of 0.09%).

Error source	C_{11}	C_{12}	C_{13}	C_{33}	C_{44}	C_{66}	e_{15}	e_{31}	e_{33}
Δf (0.06%)	0.03	0.10	0.02	< 0.01	< 0.01	< 0.01	0.67	37.7	3.6
$\Delta\rho$ (0.09%)	0.09	0.09	0.09	0.09	0.09	0.09	0.04	0.10	0.04
Δd (+1 μm in edge lengths)	< 0.01	0.07	0.19	0.08	0.02	0.05	4.8	79.3	9.4

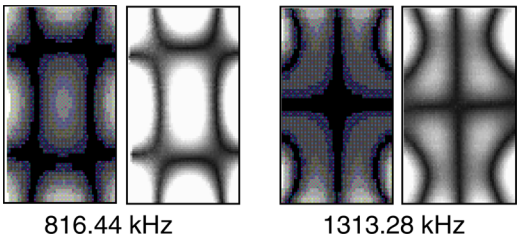

FIG. 3. (Color online) Comparison of computed (left) and measured (right) surface displacement distributions at two resonance frequencies.

are usually unknown. Mode misidentification leads to physically meaningless coefficients. We solve this by visualizing the surface displacement distribution at resonance using LDI.[17] A specimen is put on the tripod needle transducers and is kept vibrating at a resonance frequency. A He-Ne laser beam is focused on the specimen surface. The reflected light enters the Doppler interferometer. The frequency of the reflected light changes depending on the normal component of the vibration velocity through the Doppler effect. The amplitude of the velocity is proportional to the displacement because of harmonic oscillation. Scanning the specimen surface provides an image of the surface displacement distribution. Figure 3 compares computed and measured displacement distribution patterns at two resonance frequencies. Dark regions and bright regions indicate node and antinode, respectively. They show an excellent agreement, which ensures that unmistakable mode identification is achieved.

Anelastic coefficient Q_{ij}^{-1} is defined as the ratio of imaginary to real parts of the complex elastic stiffness,[29]

$$\tilde{C}_{ij} = C_{ij}\left(1 + \mathrm{i}Q_{ij}^{-1}\right). \tag{4}$$

The independent components are inversely determined from the Q^{-1} values of many vibrational modes using the calculated contribution of each internal friction component to the observed values.[21] The Q^{-1} value of each resonance peak was determined from its half-maximum peak width.

TABLE II. Elastic C_{ij} (GPa), piezoelectric e_{ij} (C/m^2), and anelastic Q_{ij}^{-1} ($\times 10^{-5}$) coefficients of wurtzite GaN. The values in parentheses are calculation results. We determined the coefficients for two crystals whose carrier density was 2.2×10^{17} and 9.3×10^{17} cm^{-3}. We define their average values as the coefficients of the wurtzite GaN.

	C_{11}	C_{12}	C_{13}	C_{33}	C_{44}	C_{66}	e_{15}	e_{31}	e_{33}	
2.2×10^{17}	361.2 ± 0.4	130.9 ± 0.4	93.1 ± 0.5	390.3 ± 0.9	98.0 ± 0.2	115.2 ± 0.1	0.12 ± 0.05	0.07 ± 0.10	0.28 ± 0.05	Present (RUS/LDI)
9.3×10^{17}	357.5	127.5	90.8	389.5	98.0	115.0	0.08	0.27	0.30	Present (RUS/LDI)
Average	359.4	129.2	92.0	389.9	98.0	115.1	0.10	0.17	0.29	Present (RUS/LDI)
	296	130	158	267	24.1	83				Mean square displacement with x-ray[a]
	390	145	106	398	105	123				Brillouin scattering[b]
	374	106	70	379	101	134				Brillouin scattering[c]
	365	135	114	381	109	115				Brillouin scattering[d]
	377	160	114	209	81.4	109				Resonance ultrasound spectroscopy (RUS)[e]
	370	145	110	390	90	113				Surface acoustic wave (SAW)[f]
	373	141	80.4	387	93.6	118				Brillouin scattering[g]
	(396)	(144)	(100)	(392)	(91)	(126)				First-principles calculation[h]
	(350)	(140)	(104)	(376)	(101)	(115)		(−0.32)	(0.63)	First-principles calculation[i]
	(367)	(135)	(103)	(405)	(95)	(116)				First-principles calculation[j]
	(334)	(132)	(99)	(372)	(86)	(101)		(−0.45)	(0.76)	First-principles calculation[k]
							−0.3	−0.36	1	Surface acoustic wave (SAW)[l]
								–0.55	1.12	Laser interferometry[m]
								(−0.49)	(0.73)	First-principles calculation[n]
2.2×10^{17}	4.7 ± 1.1	10.3 ± 3.0	8.1 ± 2.6	1.6 ± 0.4	2.3 ± 0.2	1.5 ± 0.1				Present, Q_{ij}^{-1}
9.3×10^{17}	7.3	19.1	10.3	1.7	2.5	0.8				Present, Q_{ij}^{-1}
Average	6.0	14.7	9.2	1.6	2.4	1.2				Present, Q_{ij}^{-1}

[a]Reference 6.
[b]Reference 7.
[c]Reference 8.
[d]Reference 9.
[e]Reference 11.
[f]Reference 12.
[g]Reference 10. Since C_{ij} does not satisfy $C_{12} = C_{11} - 2C_{66}$, C_{12} could be 137 GPa.
[h]Reference 30.
[i]Reference 31.
[j]Reference 32.
[k]Reference 33.
[l]References 13 and 14.
[m]Reference 15.
[n]Reference 34.

TABLE III. Diagonal components of internal friction tensor of GaN, quartz, langasite, and TeO_2 ($\times 10^{-5}$).

	Q_{11}^{-1}	Q_{33}^{-1}	Q_{44}^{-1}	Q_{66}^{-1}
GaN	6.0	1.6	2.4	1.2
Quartz[a]	1.1	1.6	4.0	3.0
Langasite[b]	17.3	9.5	2.6	2.7
TeO_2[c]	6.0	6.0	7.7	12.8

[a]Reference 20.
[b]Reference 21.
[c]Reference 23.

III. RESULTS AND DISCUSSION

Elastic, anelastic, and piezoelectric coefficients are shown in Table II together with previously reported values.[6–14,30–34] In the RUS/LDI, more than 67 resonance frequencies, up to 1670 kHz, were analyzed. For the coefficients of $2.2 \times 10^{17}\,\mathrm{cm}^{-3}$ crystal, fluctuations among four samples are shown. The fluctuations were of the same order of the measurement error described in Table I. On the other hand, differences between two crystals were larger than the fluctuations. These results indicate that C_{ij} and e_{ij} in a crystal are uniform within the measurement errors, but they vary for different crystals. We then deduced the average coefficients as the C_{ij} and e_{ij} of wurtzite GaN.

Among the reported experimental values, the mean square displacement and the RUS deduced smaller diagonal components than others. Their values were also different from the present RUS/LDI, and they appear less reliable. Except for those values, the fluctuation of the reported C_{ij} ranged from 2 to 20%. In particular, the off-diagonal components, C_{12} and C_{13}, showed large fluctuations of 12 and 20%, respectively. Comparing with the reported values, our values are somewhat small. This trend is explained by the lack of consideration of the piezoelectric stiffening in the previous studies. Regarding e_{ij}, e_{33} was smaller than the reported values, and e_{15} showed the opposite sign to the reported value. For e_{31}, both positive and negative values were observed in the specimens from $2.2 \times 10^{17}\,\mathrm{cm}^{-3}$ crystal. This large fluctuation was inevitable due to its small contribution to the resonance frequencies. As the result, we consider that the differences between obtained and reported values originate from the lack of the piezoelectric stiffening and large measurement errors in the previous studies. Thus, we deduced a new set of C_{ij} and e_{ij} that were determined with considering the piezoelectric stiffening and with lower measurement error than the other methods.

Table III shows the diagonal components of Q_{ij}^{-1} of GaN, quartz,[20] langasite,[21] and TeO_2.[23] In quartz, langasite, and TeO_2, phonon-phonon interactions were the primary factor of the internal friction.[20,21,23] Acoustic waves break an equilibrium state of phonons, due to the lattice anharmonicity. The scattered thermal-mode phonons subsequently equilibrate by interacting with a low-frequency-mode phonon and other thermal-mode phonons, during which energy loss arises. Positive relation between Q_{ij}^{-1} and temperature derivative of C_{ij} was confirmed as the proof of the primary contribution of the phonon-phonon interactions. For GaN, anisotropy between Q_{11}^{-1} and Q_{33}^{-1} is making us consider another factor affecting Q_{ij}^{-1}. In GaN, threading dislocations with line direction along $\langle 0001 \rangle$ exist.[35] Such dislocation contributes attenuation on vibrational deformation around the $\langle 0001 \rangle$ direction. Q_{11}^{-1} is larger than Q_{33}^{-1} by a factor of 3.75, and such a high anisotropy has not been observed in other piezoelectric materials. This may be related with the dislocation damping by the threading dislocation: the in-plane deformation may cause the anelastic motions of those dislocations.

IV. CONCLUSIONS

Elastic, anelastic, and piezoelectric coefficients of wurtzite GaN were determined by the RUS/LDI. Our values were different from those previously reported. Considering the fluctuation of the coefficients among the specimens, reliable values were obtained for the elastic coefficients, though the piezoelectric coefficients showed large fluctuation. In anelastic coefficients, we found pronounced anisotropy between Q_{11}^{-1} and Q_{33}^{-1}.

ACKNOWLEDGMENTS

Authors acknowledge cooperation of Mitsubishi Chemical Corporation.

[1]*Semiconductors*, Landolt-Börnstein, New Series, Group III (Springer, Berlin, 1999), Vol. 41A1β.
[2]S. H. Lee, H. H. Jeong, S. B. Bae, H. C. Choi, J. H. Lee, and Y. H. Lee, IEEE Trans. Electron Devices **48**, 524 (2001).
[3]R. C. Woods and F. A. Boroumand, IEEE Trans. Electron Devices **53**, 173 (2006).
[4]Y. Kuwahara, T. Fujii, T. Sugiyama, D. Iida, Y. Isobe, Y. Fujiyama, Y. Morita, M. Iwaya, T. Takeuchi, S. Kamiyama, I. Akasaki, and H. Amano, Appl. Phys. Express **4**, 021001 (2011).
[5]B. A. Auld, *Acoustic Fields and Waves in Solids* (Wiley, New York, 1973).
[6]V. A. Savastenko and A. U. Sheleg, Phys. Status Solidi A **48**, K135 (1978).
[7]A. Polian, M. Grimsditch, and I. Grzegory, J. Appl. Phys. **79**, 3343 (1996).
[8]Y. Takagi, M. Ahart, T. Azuhata, T. Sota, K. Suzuki, and S. Nakamura, Physica B **219-220**, 547 (1996).
[9]M. Yamaguchi, T. Yagi, T. Azuhata, T. Sota, K. Suzuki, S. Chichibu, and S. Nakamura, J. Phys.: Condens. Matter **9**, 241 (1997).
[10]T. Deguchi, D. Ichiryu, K. Toshikawa, K. Sekiguchi, T. Sota, R. Matsuo, T. Azuhata, M. Yamaguchi, T. Yagi, S. Chichibu, and S. Nakamura, J. Appl. Phys. **86**, 1860 (1999).
[11]R. B. Schwarz, K. Khachaturyan, and E. R. Weber, Appl. Phys. Lett. **70**, 1122 (1997).
[12]C. Deger, E. Born, H. Angerer, O. Ambacher, M. Stutzmann, J. Hornsteiner, E. Riha, and G. Fischerauer, Appl. Phys. Lett. **72**, 2400 (1998).
[13]A. D. Bykhovski, B. L. Gelmont, and M. S. Shur, J. Appl. Phys. **81**, 6332 (1997).
[14]G. D. O'Clock, Jr. and M. T. Duffy, Appl. Phys. Lett. **23**, 55 (1973).
[15]I. L. Guy, S. Muensit, and E. M. Goldys, Appl. Phys. Lett. **75**, 4133 (1999).
[16]C. M. Lueng, H. L. W. Chan, C. Surya, and C. L. Choy, J. Appl. Phys **88**, 5360 (2000).
[17]H. Ogi, K. Sato, T. Asada, and M. Hirao, J. Acoust. Soc. Am. **112**, 2553 (2002).
[18]I. Ohno, Phys. Chem. Miner. **17**, 371 (1990).
[19]M. Dunn, H. Ledbetter, and P. Heyliger, *Engineering Mechanics* (ASME, Washington, 1995), p. 758.
[20]H. Ogi, T. Ohmori, N. Nakamura, and M. Hirao, J. Appl. Phys. **100**, 053511 (2006).
[21]H. Ogi, N. Nakamura, K. Sato, M. Hirao, and S. Uda, IEEE Trans. Ultrason. Ferroelectr. Freq. Control **50**, 553 (2003).

[22]H. Ogi, Y. Kawasaki, M. Hirao, and H. Ledbetter, J. Appl. Phys. **92**, 2451 (2002).
[23]H. Ogi, M. Fukunaga, M. Hirao, and H. Ledbetter, Phys. Rev. B **69**, 024104 (2004).
[24]R. Bechmann, Phys. Rev. **110**, 1060 (1958).
[25]Y. Ohashi, M. Arakawa, J. Kushibiki, B. M. Epelbarum, and A. Winnacker, Appl. Phys. Express **1**, 077004 (2008).
[26]A. S. Barker, Jr. and M. Ilegems, Phys. Rev. B **7**, 743 (1973).
[27]D. D. Manchon, Jr., A. S. Barker, Jr., P. J. Dean, and R. B. Zetterstrom, Solid State Commun. **8**, 1227 (1970).
[28]H. H. Demarest, Jr., J. Acoust. Soc. Am. **49**, 768 (1971).
[29]H. Ledbetter, C. Fortunko, and P. Heyliger, J. Mater. Res. **10**, 1352 (1995).
[30]K. Kim, W. R. L. Lambrecht, and B. Segall, Phys. Rev. B **53**, 16310 (1996).
[31]K. Shimada, T. Sota, and K. Suzuki, J. Appl. Phys. **84**, 4951 (1998).
[32]A. F. Wright, J. Appl. Phys. **82**, 2833 (1997).
[33]Y. Duan, J. Li, S. Li, and J. Xia, J. Appl. Phys. **103**, 023705 (2008).
[34]F. Bernardini, V. Fiorentini, and D. Vanderbilt, Phys. Rev. B **56**, R10024 (1997).
[35]Y. Xin, S. J. Pennycook, N. D. Browning, P. D. Nellist, S. Sivananthan, F. Omnès, B. Beaumont, J. P. Faurie, and P. Gibart, Appl. Phys. Lett. **72**, 2680 (1998).